Physica B 485 (2016) 94–102

Contents lists available at ScienceDirect

Physica B

journal homepage: www.elsevier.com/locate/physb

Green's functions of the scalar model of electromagnetic fields in sinusoidal superlattices

V.A. Ignatchenko *, D.S. Tsikalov

L.V. Kirensky Institute of Physics, Siberian Branch of RAS, 660036 Krasnoyarsk, Russia

ARTICLE INFO

Article history:
Received 5 August 2015
Received in revised form
25 December 2015
Accepted 7 January 2016
Available online 14 January 2016

Keywords:
Green's functions
Electromagnetic waves
Scalar model
Sinusoidal superlattices
Photonic crystals
LDOS

ABSTRACT

Problems of obtaining Green's function and using it for studying the structure of scalar electromagnetic fields in a sinusoidal superlattice are considered. An analytical solution of equation in the **k**-space for Green's function is found. Green's function in the **r**-space is obtained by both the numerical and the approximate analytical Fourier transformation of that solution. It is shown, that from the experimental study of Green's function in the **k**-space the position of the plane radiation source relative to the extremes of the dielectric permittivity $\varepsilon(z)$ can be determined. The relief map of Green's function in the **r**-space shows that the structure of the field takes the form of chains of islets in the plane ωz, the number of which increases with increasing the distance from a radiation source. This effect leads to different frequency dependences of Green's function at different distances from the radiation source and can be used to measure the distance to the internal source. The real component of Green's function and its spatial decay in the forbidden zones in the near field is investigated. The local density of states, depending on the position of the source in the superlattice, is calculated.

© 2016 Elsevier B.V. All rights reserved.

1. Introduction

Photonic crystals, which are artificially created media with periodic physical parameters, has recently been widely studied (see, e.g., Refs. [1–6]). Knowledge of analytical expressions for Green's function of waves propagating in such media, is necessary when considering a number of problems, both theory and experiment. Green's function in the coordinate space $G(\omega, \mathbf{r}, \mathbf{r}_0)$ is used as in dealing with problems related to the structure of wave fields in periodic media and computing the most important characteristics such as the local density of states (LDOS) [7–10]. Green's function in the wave vector space $G(\omega, \mathbf{k}, \mathbf{r}_0)$ is needed in the study of various aspects of theory, for example, the theory of wave scattering by inhomogeneities [11,12]. The wave equation for Green's function in one-dimensional superlattice, periodic along the z-axis, is reduced to a one-dimensional equation by the Fourier transformation in the $\xi = x - x_0$ and $\zeta = y - y_0$ coordinates. This work is devoted to finding and investigating Green's functions for the scalar model of electromagnetic waves in one-dimensional superlattice with a sinusoidal profile of modulation of the dielectric permittivity $\varepsilon(z)$. Real photonic crystals typically have a modulation profile $\varepsilon(z)$, nearly rectangular. A number of physical phenomena occurring in the propagation of waves in periodic media, are very sensitive to the shape of the profile of $\varepsilon(z)$. However, a number of phenomena, including the fundamental nature, are qualitatively similar for all periodic profiles of $\varepsilon(z)$. The sinusoidal modulation of $\varepsilon(z)$ is the most suitable for the analytical study of such phenomena. A homogeneous equation for a sinusoidal superlattice (Mathieu equation) is well studied (see, e.g., Ref. [13]). Green's function of waves in this superlattice is much less studied. In Refs. [14–18], approximate expressions for Green's function in the coordinate space $G(\omega, \mathbf{r}, \mathbf{r}_0)$ have been found and studied.

The objectives of this paper are: (i) obtaining an analytical representation of Green's function in **k**-space $G(\omega, \mathbf{k}, \mathbf{r}_0)$ for scalar waves in the one-dimensional sinusoidal superlattice; (ii) the numerical and approximate analytical representation of this function in the **r**-space $G(\omega, \mathbf{r}, \mathbf{r}_0)$; (iii) investigation of the structure of the scalar fields of the plane radiation source using both forms of Green's function, $G(\omega, \mathbf{k}, \mathbf{r}_0)$ and $G(\omega, \mathbf{r}, \mathbf{r}_0)$.

2. Solution of Green's function equation

Green's function of scalar model of electromagnetic waves in a sinusoidal superlattice satisfies the equation

$$\nabla^2 G(\mathbf{r}, \mathbf{r}_0) + \left[\nu + 2\eta \cos(qz + \psi)\right] G(\mathbf{r}, \mathbf{r}_0) = -\delta(\mathbf{r} - \mathbf{r}_0), \quad (1)$$

where $\nu = \varepsilon(\omega/c)^2$, $2\eta = \Delta\varepsilon(\omega/c)^2$, $q = 2\pi/l$; ω and c are the

* Corresponding author.
E-mail address: vignatch@iph.krasn.ru (V.A. Ignatchenko).

http://dx.doi.org/10.1016/j.physb.2016.01.006
0921-4526/© 2016 Elsevier B.V. All rights reserved.

frequency and the speed of light in vacuum, respectively; ε and $\Delta\varepsilon$, respectively, are the mean value and the amplitude of modulation of a dielectric permittivity, l and ψ are the spatial period and the phase of the superlattice, respectively. Here and below, we do not indicate explicitly the dependence of Green's functions on the frequency if it does not lead to misunderstandings. In addition to Eq. (1), Green's function must satisfy the standard conditions of radiation. Equations for scalar models of elastic and spin waves differ renaming parameters.

Since the medium is periodically inhomogeneous along the superlattice z-axis, Green's function depends not only on the difference $z - z_0$, and the z-coordinate directly. In the xy plane, Green's function depends only on the difference of the corresponding coordinates, that allows us to carry out the two-dimensional Fourier transformation in the transverse coordinates $\xi = x - x_0$ and $\zeta = y - y_0$:

$$G(\mathbf{r}, \mathbf{r}_0) = \int G(\mathbf{k}_\perp, z, z_0) \exp\left[i(\xi k_\xi + \zeta k_\zeta)\right] dk_\xi\, dk_\zeta. \tag{2}$$

The result is a one-dimensional equation in the form

$$\frac{d^2}{dz^2} G(\mathbf{k}_\perp, z, z_0) + \left[\varkappa + 2\eta \cos(qz + \psi)\right] G(\mathbf{k}_\perp, z, z_0) = -\frac{1}{(2\pi)^2}\delta(z - z_0), \tag{3}$$

where $\varkappa = \nu - k_\perp^2$ and $\mathbf{k}_\perp = \mathbf{i}k_\xi + \mathbf{j}k_\zeta$ is a two-dimensional wave vector. Eq. (3) was used in Refs. [16,18], where the approximate expressions for Green's function in some limiting cases had been obtained. In those studies, Eq. (3) was investigated in the coordinate z-space. In that case, the solution of Eq. (3) was expressed in terms of independent solutions of the corresponding homogeneous equation [13]. These cumbersome expressions are not always convenient both in analytical and numerical calculations.

In this paper, we develop another method for studying the solution of Eq. (3), which we briefly have described previously [19]. First, we find the analytical solution of Eq. (3) in k_z-space, and then examine it numerically and analytically in $\mathbf{r}$-space. Applying the Fourier transformation to Eq. (3)

$$G(z) = \int G(k_z) \exp(ik_z z)\, dk_z, \quad G(k_z) = \frac{1}{2\pi}\int G(z) \exp(-ik_z z)\, d_z, \tag{4}$$

we obtain

$$\left[\varkappa - k_z^2\right] G(k_z) + \eta\left[e^{i\psi} G(k_z - q) + e^{-i\psi} G(k_z + q)\right] = -\frac{1}{(2\pi)^3}\exp\left[-ik_z z_0\right]. \tag{5}$$

To find the solution of Eq. (5), we use the methods of analysis of systems of matrix equations [20,21]. Doing the corresponding operations (see Appendix A), we obtain Green's function in $\mathbf{k}$-space in a compact expression containing the ascending and ordinary continued fractions

$$G(\mathbf{k}_\perp, k_z, z_0) = -\frac{\exp(-ik_z z_0)}{(2\pi)^3}\frac{1 + P_1^+ + P_1^-}{L_0}. \tag{6}$$

Here $P_1^\pm$ are ascending continued fractions, determined by the recursive formula

$$P_n^\pm = -\eta \exp(\pm i\psi)\frac{\exp(\pm inqz_0) + P_{n+1}^\pm}{L_n^\mp}, \tag{7}$$

and L_0 and $L_n^\pm$ are ordinary continued fractions defined by the formulas

$$L_0 = \varkappa - k_z^2 - \eta^2\left[\frac{1}{L_1^+} + \frac{1}{L_1^-}\right], \quad L_n^\pm = \varkappa - (k_z \pm nq)^2 - \frac{\eta^2}{L_{n+1}^\pm}. \tag{8}$$

Continued fractions in Eq. (6) have fast convergence, so that expression is useful in the study of Green's function in $\mathbf{k}$-space and in the $\mathbf{r}$-space. In some cases it is convenient to use also the expansion of Green's function in a Fourier series, which has the form

$$G(\mathbf{k}_\perp, k_z, z_0) = \sum_{n=-\infty}^{\infty} g_{\mathbf{k}}^n \exp\left[-i(k_z - nq)z_0\right]. \tag{9}$$

Here the factors $g_{\mathbf{k}}^n$ are determined by the expression

$$g_{\mathbf{k}}^{\pm n} = -\frac{1}{(2\pi)^3}\left[-\eta \exp(\pm i\psi)\right]^n \Big/ L_n^\mp \Big/ L_{n-1}^\mp \Big/ \cdots \Big/ L_0, \quad n = 0, 1, 2, \ldots, \tag{10}$$

where continued fractions designated by slash characters.

3. Field structures of a plane radiation source

In what follows, all graphs of Green's functions correspond to the plane radiation source located in the plane xy. Green's function of the source in the z-space defined by the equation

$$G(z, z_0) = \iint G(\mathbf{r}, \mathbf{r}_0)\, dx_0\, dy_0. \tag{11}$$

Substituting Eq. (2) into Eq. (11) and integrating over x_0 and y_0, we obtain

$$G(z, z_0) = (2\pi)^2 \iint G(\mathbf{k}_\perp, z, z_0)\exp\left[i(xk_\xi + yk_\zeta)\right]\delta(k_\xi)\delta(k_\zeta)\, dk_\xi\, dk_\zeta = (2\pi)^2 G(\mathbf{k}_\perp, z, z_0)|_{\mathbf{k}_\perp = 0}. \tag{12}$$

It follows that Green's functions of a plane source $G(k_z, z_0)$ and $G(z, z_0)$ related to the general expression for the spectral form of Green's function, Eq. (6), by the following relations:

$$G(k_z, z_0) = (2\pi)^2 G(\mathbf{k}_\perp, k_z, z_0)|_{\mathbf{k}_\perp = 0}, \tag{13}$$

$$G(z, z_0) = (2\pi)^2 \int G(\mathbf{k}_\perp, k_z, z_0)\Big|_{\mathbf{k}_\perp = 0} \exp(ik_z z)\, dk_z. \tag{14}$$

Examples of relief maps of the imaginary part of Green's function $G''(\omega, k_z)$ in k_z-space calculated by Eqs. (6) and (13) are shown in Fig. 1 for the three phase values: $\psi = 0$ (a), $\pi/2$ (b), and π (c). For the expressiveness of maps, the dimensionless factor ω/ω_r is added to the normalization of Green's functions, where ω_r corresponds to the middle frequency of the first forbidden Brillouin zone of the superlattice. Without such a leveling factor, the amplitudes of the relief in the high-Brillouin zones are too small. In the calculations, it is assumed that the source coordinate $z_0 = 0$ and the location of the source relative to the superlattice is governed by the spatial phase of the superlattice ψ. Phase $\psi = 0$ corresponds to the source position in one of the maxima of the function $\cos qz$, i.e., in a center of the layer with a large value of ε, the phase $\psi = \pi/2$ corresponds to the source position at the boundary between the layers, and the phase $\psi = \pi$ corresponds to the source position in a center of the layer with a lower value of ε (see the image of a superlattice in the bottom of Fig. 2). In the color version of Fig. 1, available online, one can see that the phase change leads to radical restructuring the relief of the function $G''(\omega, k_z)$. At the sites of some positive for $\psi = 0$ peaks of this function, the negative peaks occur at $\psi = \pi$, the character of the sequence of peak sights changes as along the k_z coordinate, and along the ω coordinate. Especially peculiar pattern corresponds to the phase $\psi = \pi/2$, when instead of peaks the curves having both positive and negative components occur.

The spatial structure of the electromagnetic field in the superlattice along the z-axis describes by Green's function $G(\omega, z)$. This function is determined by the Fourier transformation in the

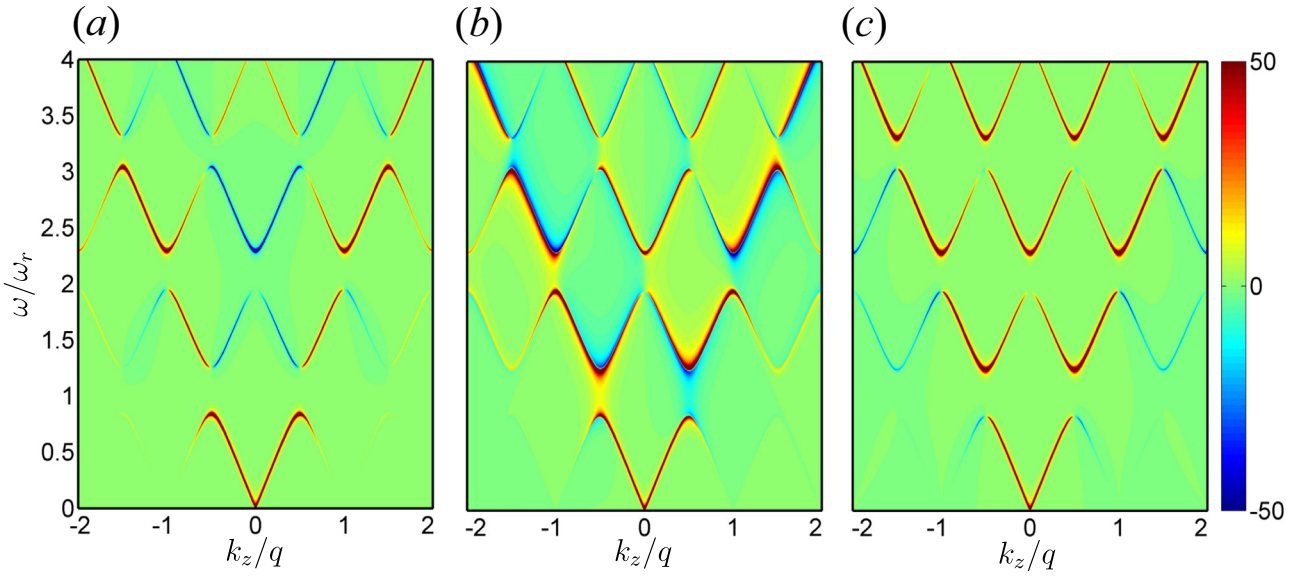

Fig. 1. Relief maps of the imaginary part of the normalized Green's function $2\pi(\omega/\omega_r)q^2G(\omega, k_z)$ for various values of the superlattice phase $\psi = 0$ (a), $\pi/2$ (b) and π (c). The relative modulation of the dielectric permittivity $\Delta\varepsilon/\varepsilon = 0.8$. The attenuation $\omega''/\omega_r = 0.01$ was introduced in the calculations. The source is at $z_0 = 0$ as here and in all following figures. (For interpretation of the references to color in this figure caption, the reader is referred to the web version of this paper.)

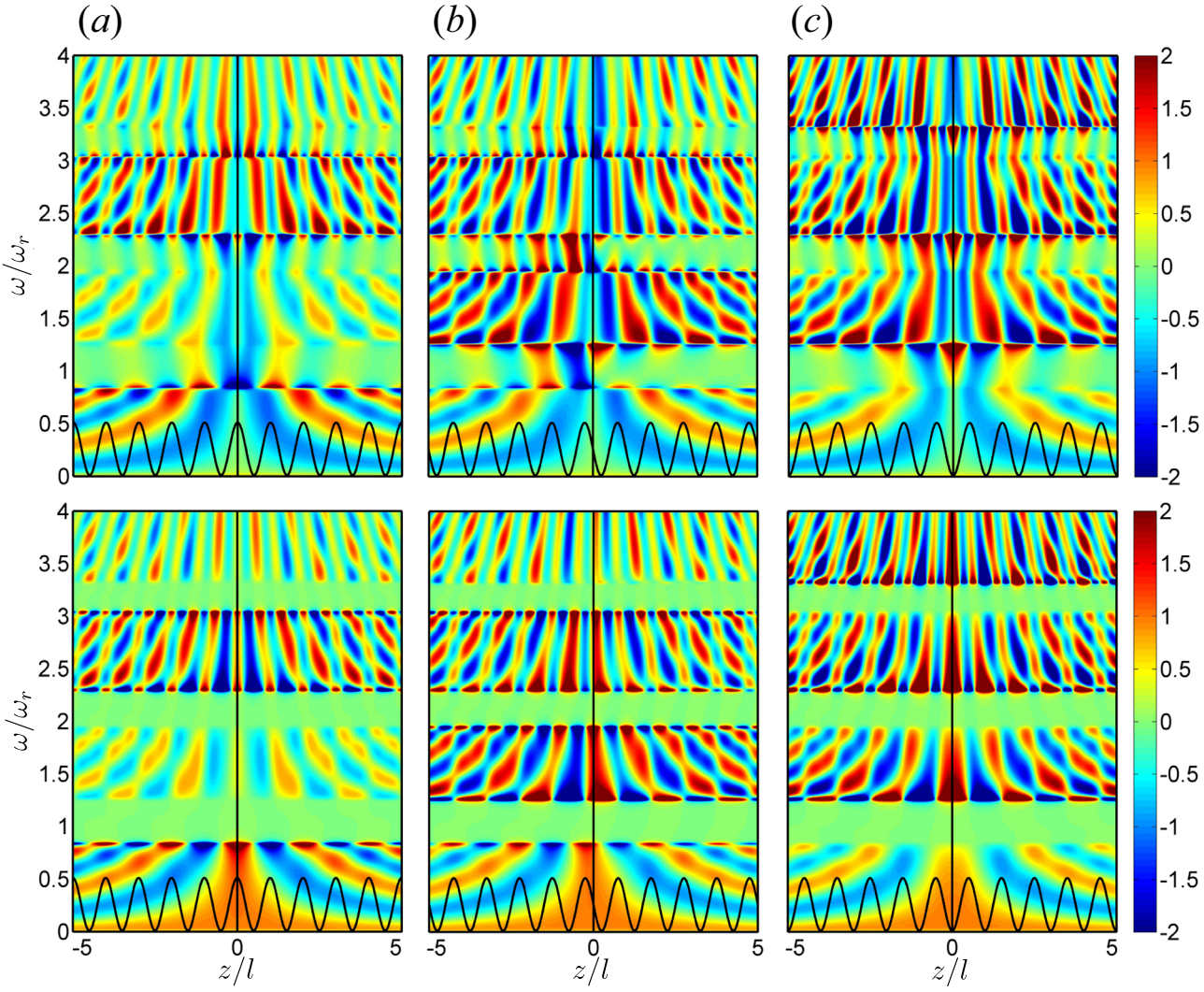

Fig. 2. Relief maps of the real (top) and the imaginary (bottom) parts of the normalized Green's function $(\omega/\omega_r)qG(\omega, z)$ for various values of the superlattice phase $\psi = 0$ (a), $\pi/2$ (b) and π (c). At the bottom of each of the drawings (a), (b) and (c), the position of the superlattice corresponding to this phase is shown. $\Delta\varepsilon/\varepsilon = 0.8$, $\omega''/\omega_r = 0.01$. (For interpretation of the references to color in this figure caption, the reader is referred to the web version of this paper.)

projection of the wave vector k_z of the spectral representation of Green's function $G''(\omega, k_z)$, Eqs. (6) and (14). This transformation can not be done analytically because of the very complex dependence of expressions $P_1^{\pm}$, L_0, and L_n on k_z. Therefore, the Fourier transformation in Eq. (14) was carried out numerically. When performing this transformation should take into account the radiation conditions.

Relief maps of the real and imaginary parts of Green's function $G(\omega, z)$ are shown in Fig. 2 for the three phase values: $\psi = 0$ (a), $\pi/2$ (b), and π (c). In the normalization of Green's functions, as well as in Fig. 1, the factor ω/ω_r added to increase the intensity of amplitudes in high-frequency areas of the spectrum. The source is at $z_0 = 0$. At the bottom of each of the drawings a, b and c, the position of the superlattice corresponding to this phase is shown. It is seen that for $\psi = 0$ and π the relief is symmetric with respect to the position of the source, and when $\psi = \pi/2$ it has a pronounced asymmetry. The part of the relief of Green's function $G(\omega, z)$, situated lower of the first gap, is compared with the relief calculated by the approximate analytical expression obtained for this case early [16]. Both reliefs in this area are in good agreement with each other.

Fig. 2 shows the dramatic change in the electromagnetic field in the superlattice with increasing the distance from the source. The character of this change is the same for both imaginary and real part of Green's function. Lines of zeros of the function at some points come nearer to each other and the chains of islets on the relief map of the function $G(\omega, z)$ are formed in the plane ωz. With z increasing the size of the islands decreases, the number of them increases and chains tilt to the z-axis.

Cardinal restructuring of the electromagnetic field occurs when the superlattice phase changes relative to the position of the source. In the color version of Fig. 2, available on-line, can be seen as with changing the phase, the maxima in the function $G(\omega, z)$ appear in places of minima and vice versa. The imaginary part of Green's function $G''(\omega, z)$ in the band gap is completely absent as for far and near field (present on the graphs of small amplitude is due to attenuation introduced in the calculations). The amplitudes of the real part of Green's function are present in the band gap only in the near field. As the distance from the source increases, these amplitudes decay.

Fig. 3 shows in more detail the change in the frequency dependence of the imaginary part of Green's function $G''(\omega, z)$ when observing it at different fixed distances from the source $z=2l$, $3l$ and $4l$. Green's functions are shown in the frequency range corresponding to the width of the second Brillouin zone and at the location of the source in the minimum of the function $\varepsilon(z)$ (i.e., for $\psi = \pi$). It is seen that with increasing the distance z for one period, radical restructuring the depending of the function $G''(\omega, z)$ on ω occurs: the number of extrema and the number of zeros of this function increase for a unit. Even small compared with the period of the superlattice the change in z leads to a rather pronounced changes in the frequency dependence of the function $G''(\omega, z)$. Thus, the observation of the depending of the function $G'(\omega, z)$ or $G''(\omega, z)$ on the frequency allows you to measure the distance between the planar source and the plane of observation with an accuracy of a fraction of a wavelength. One more method of measuring the thickness of one-dimensional photonic crystals can be developed on this principle.

The experimentally often quantities are studied that are not proportional to the intensity G, but the radiation power $|G^2|$. The distribution coefficient of the radiation power in the superlattice is characterized by

$$K(\omega, z) = |G(\omega, z)|^2/|G_0(\omega, z)|^2, \tag{15}$$

where $G_0(\omega, z)$ is the Green's function of free space. In Fig. 4 a relief

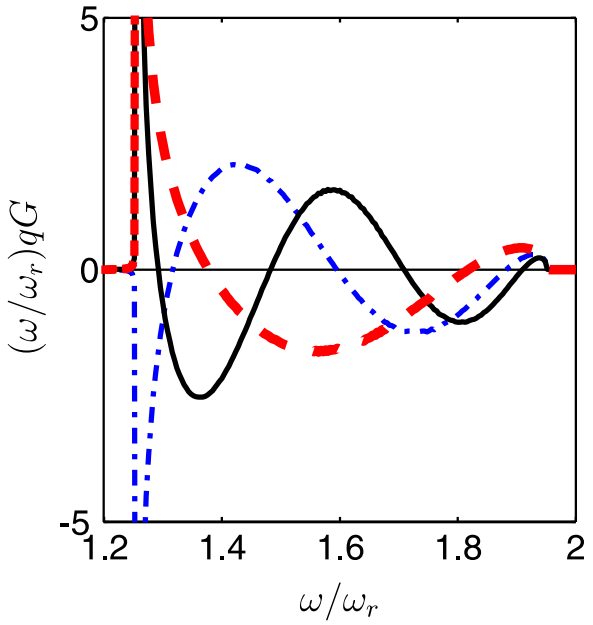

Fig. 3. Frequency dependences of the normalized imaginary part of Green's function $(\omega/\omega_r)qG(\omega, z)$ in the second Brillouin zone at different fixed distances from the source $z=2l$ (dashed curve, the red), $3l$ (dot-dashed curve, blue), and $4l$ (solid curve, black). $\Delta\varepsilon/\varepsilon = 0.8$, $\omega''/\omega_r = 10^{-4}$. (For interpretation of the references to color in this figure caption, the reader is referred to the web version of this paper.)

of the function $K(\omega, z)$ is shown that we calculated for the same parameters of the superlattice, which in Fig. 2 shows the relief maps of the real $G'(\omega, z)$ and imaginary $G''(\omega, z)$ parts of Green's function. Comparison of these figures with each other shows a dramatic qualitative difference the structure of the spectra both $G'(\omega, z)$ and $G''(\omega, z)$, on the one hand and the structure of the spectrum of $K(\omega, z)$, on the other hand. For the functions $G'(\omega, z)$ and $G''(\omega, z)$ are characteristic the structure of chains of islets that with increasing z increasingly tilted to the z-axis. For $K(\omega, z)$, the repetitive structure of cells, oriented perpendicular to the z-axis is observed. Fig. 5 illustrates how such a dramatic transformation of the structure and symmetry of the fields takes place. Eq. (15) can be written as

$$K(\omega, z) = \left[\frac{|G'(\omega, z)|^2}{|G_0(\omega, z)|^2}\right] + \left[\frac{|G''(\omega, z)|^2}{|G_0(\omega, z)|^2}\right]. \tag{16}$$

Fig. 5 shows the frequency dependence of squares of the imaginary $G''(\omega, z)$ (dashed lines, red) and real $G'(\omega, z)$ (dot-dashed lines, green) parts of Green's function for the values of the coordinates $z=2l$, $3l$ and $4l$. These squares, as well as themselves functions $G''(\omega, z)$ and $G'(\omega, z)$ (see Fig. 3), have the form of curves with different number of maxima along the ω axis for the different fixed values of z. However, the maxima and minima of squares of the functions $G'(\omega, z)$ and $G''(\omega, z)$ in the summation are mutually compensated and their sums (solid lines, black) have the form of smooth curves with a single maximum, the shape of which is practically independent of z. Thus, an islet structure of the field, discovered in this study is a phase effect: the effect disappears in the calculation (or measurement) of the module of Green's function. The measurement of $K(\omega, z)$ instead of $G'(\omega, z)$ or $G''(\omega, z)$ results in a significant loss of information. In particular, it is impossible to measure the distance to the radiation source from the frequency dependence of $K(\omega, z)$ at a fixed z.

The most important characteristic of inhomogeneous media is the LDOS [7–10]:

$$\rho_l(\omega, \mathbf{r}_0) = \frac{2\omega}{\pi c^2}\mathrm{Im}\big[G(\omega, \mathbf{r}_0, \mathbf{r}_0)\big]. \tag{17}$$

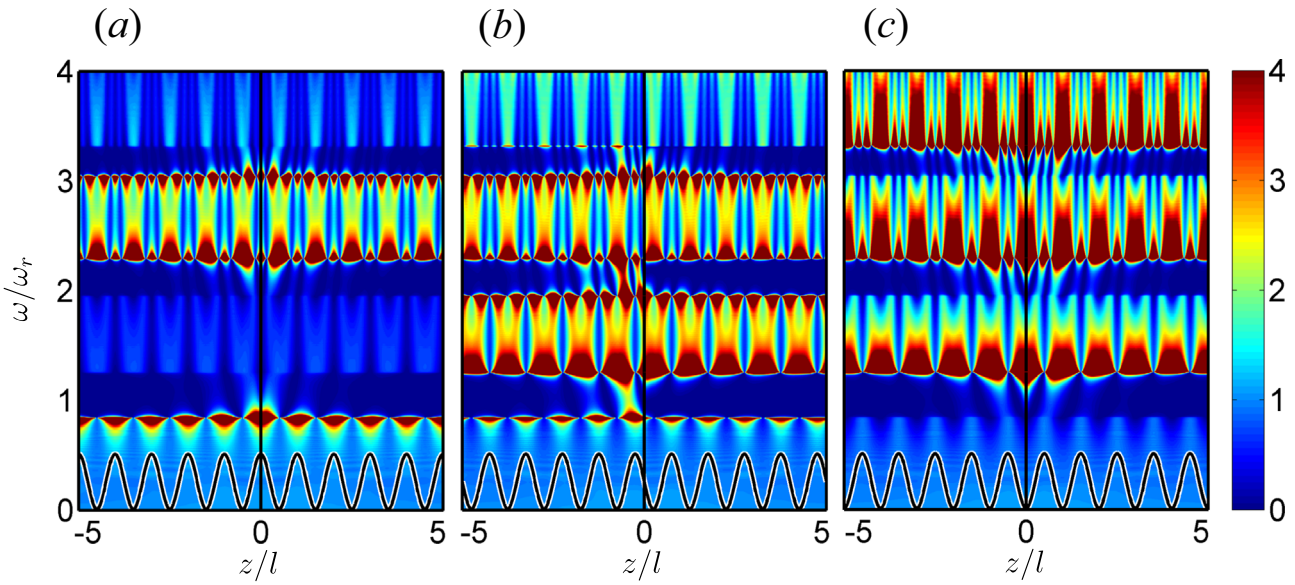

Fig. 4. The relief map of the normalized radiation power $K(\omega, z)$ for various values of the superlattice phase $\psi = 0$ (a), $\pi/2$ (b) and π (c). $\Delta\varepsilon/\varepsilon = 0.8$, $\omega''/\omega_r = 10^{-4}$.

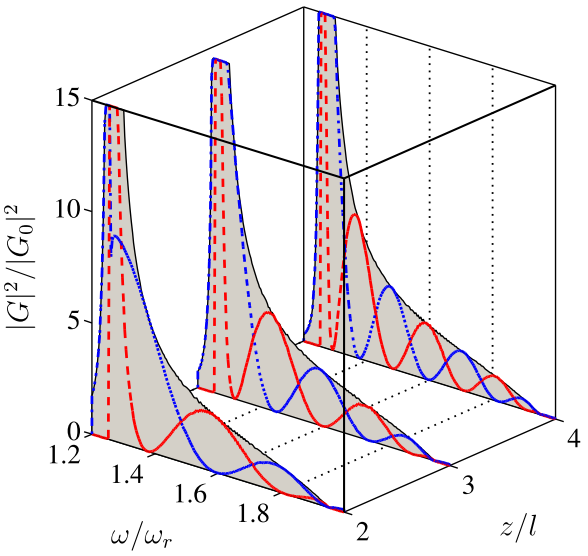

Fig. 5. Frequency dependencies of normalized squares of the imaginary (dashed lines, red) and the real (dotted curves, blue) parts of Green's function, and their sum K (solid lines, black) at distances from the source $z=2l$, $3l$ and $4l$. $\Delta\varepsilon/\varepsilon = 0.8$, $\omega''/\omega_r = 10^{-4}$. (For interpretation of the references to color in this figure caption, the reader is referred to the web version of this paper.)

The function of the LDOS for a plane source in a sinusoidal superlattice has calculated by us in the coordinates ω and ψ (Fig. 6). It is assumed, as in the relief map of Green's function (Figs. 1 and 2), that the plane source is located at the point $z = z_0$, and its position relative to the superlattice is characterized by the superlattice phase ψ. Thus, $\psi = 0$ corresponds to the position of the source in the maximum value of the function $\varepsilon(z)$ and $\psi = \pi$ and $\psi = -\pi$ correspond to the minimum of the function. Relief map of the normalized function ρ_l/ρ_0, where ρ_0 is the LDOS for a plane source in vacuum, are shown in Fig. 6a for four Brillouin zones. Dependences of the function ρ_l/ρ_0 on ψ at fixed frequencies are shown in Fig. 6b for three Brillouin zones ($n=1$, 2 and 3). Solid lines at $n=2$ and 3 correspond to the frequencies near the lower edge of the corresponding band, and at $n=1$ to the middle of the first zone. Dashed curves in all three figures correspond to frequencies near the upper edge of each zone. The LDOS for a superlattice with the rectangular profile of the function $\varepsilon(z)$ was calculated in Ref. [7] for the third Brillouin zone. That function differs from the function in Fig. 6b, $n=3$, by the presence of sharp jumps at points corresponding to the interfaces between layers of the superlattice. A possible cause of these jumps is a large difference in the steepness of the slopes of the function $\varepsilon(z)$ for the sinusoidal and rectangular profiles of the function. However, it clearly cannot be argued, as LDOS in Ref. [7], in contrast to our work, was calculated for a superlattice with different thicknesses from each other adjacent layers. The latter fact could also lead to sharp differences of LDOS for the superlattices considered in these studies.

4. Approximate analytical representations of Green's function

In this section, an approximate expressions for the Green's function $G(\mathbf{k}_\perp, k_z, z_0)$ and $G(\mathbf{k}_\perp, z, z_0)$, which are valid in the first and second Brillouin zones of the superlattice, and the band gap between these zones, derived from the exact formula (6). The structure of the fields in these areas, in many cases, is of particular interest. In the frequency range from zero to the second gap, Eq. (6) can be approximately represented as

$$G(\omega, k_z) = -\frac{\exp(-ik_z z_0)}{(2\pi)^3} \frac{1 - \dfrac{\eta e^{i(qz_0+\psi)}}{\varkappa - (k_z - q)^2} - \dfrac{\eta e^{-i(qz_0+\psi)}}{\varkappa - (k_z + q)^2}}{\varkappa - k_z^2 - \dfrac{\eta^2}{\varkappa - (k_z - q)^2} - \dfrac{\eta^2}{\varkappa - (k_z + q)^2}}. \quad (18)$$

Transition in z-space, we perform by the method of the residue theory. The poles of the expression (Eq. (18)) are described by the biquadratic cubic equation, analytical solutions of which are cumbersome expressions. Our objective is to obtain the relatively simple analytical formulas. Eq. (18) comprises six poles. Only four of them, leading to the splitting of the dispersion curves on the boundary of the first Brillouin zone, should be taken into account: the two "non-resonant" poles should be discarded according to the approximations used in Eq. (18). This corresponds to a known provision that in a periodically inhomogeneous medium with shallow depth of modulation, the normal waves can be constructed up to the second band gap of four traveling waves with the coordinate factors of the form [22,23]

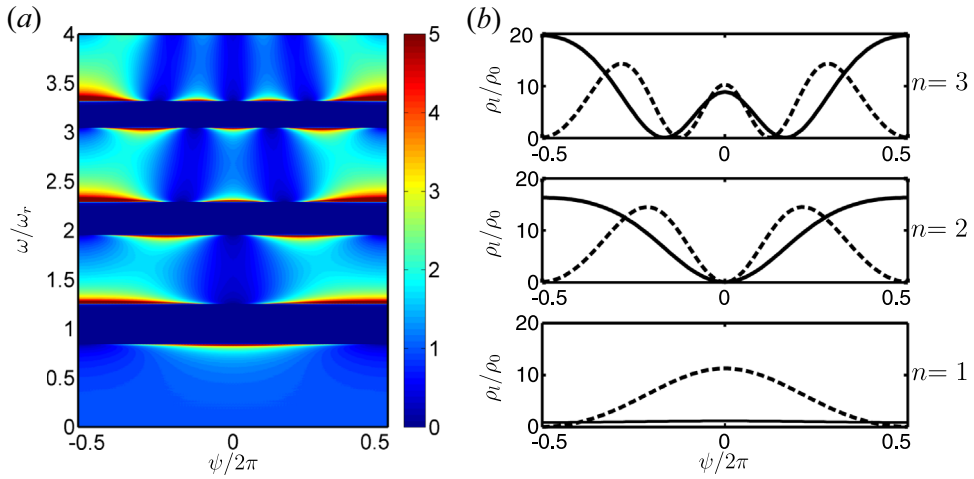

Fig. 6. Relief map of the normalized LDOS ρ_l/ρ_0, where ρ_0 is the LDOS for a plane source in vacuum (a). Dependences of the function ρ_l/ρ_0 on the superlattice phase ψ for the frequencies $\omega/\omega_r = 0.5$ (solid curve) and 0.838 (dashed curve) in the first Brillouin zone ($n=1$), $\omega/\omega_r = 1.264$ (solid curve) and 1.946 (dashed curve) in the second Brillouin zone ($n=2$), and $\omega/\omega_r = 2.304$ (solid curve) and 3.036 (dashed curve) in the third Brillouin zone ($n=3$) (b). $\Delta\varepsilon/\varepsilon = 0.8$, $\omega''/\omega_r = 10^{-3}$.

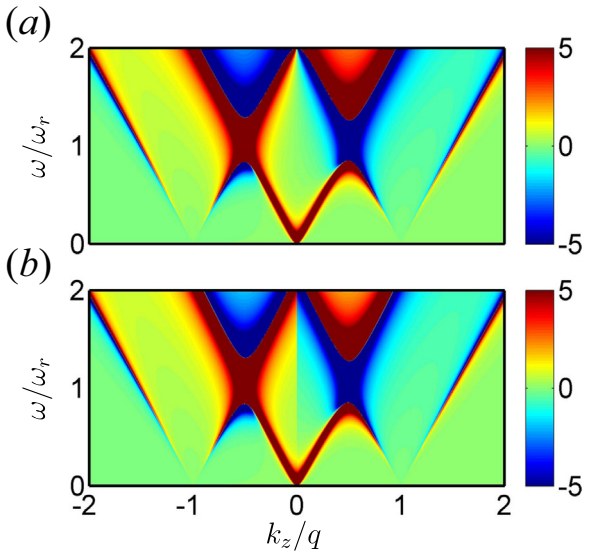

Fig. 7. Comparison of the imaginary parts of the approximate (a), Eq. (18), and modeling (b), Eq. (20), representations of Green's function $2\pi(\omega/\omega_r)q^2G(\omega, k_z)$. $\Delta\varepsilon/\varepsilon = 0.8$, $\omega''/\omega_r = 0.01$.

$$\exp\left[\pm\left(\frac{q}{2}\pm\sqrt{\varkappa+\frac{q^2}{4}-\sqrt{\varkappa q^2+\eta}}\right)iz\right]. \tag{19}$$

Based on the above comments, we propose to use for finding the poles a model function of the form

$$G(\omega, k_z) = -\frac{\exp(-ik_z z_0)}{(2\pi)^3}\frac{1-\frac{\eta e^{i(qz_0+\psi)}}{\varkappa-(k_z-q)^2}\theta(k_z)-\frac{\eta e^{-i(qz_0+\psi)}}{\varkappa-(k_z+q)^2}\theta(-k_z)}{\varkappa-k_z^2-\frac{\eta^2}{\varkappa-(k_z-q)^2}\theta(k_z)-\frac{\eta^2}{\varkappa-(k_z+q)^2}\theta(-k_z)}, \tag{20}$$

where $\theta(k_z)$ is the Heaviside function

$$\theta(k_z) = \begin{cases} 1 & k_z > 0, \\ 0 & k_z < 0. \end{cases} \tag{21}$$

Fig. 7 shows relief maps of the imaginary parts of Green's function corresponding to the approximate formula, Eq. (18), and the modeling formula, Eq. (20) for $\mathbf{k}_\perp = 0$, i.e., for a plane source. One can see a good agreement for both functions together. To notice the differences, the relief depth scale is reduced by one order of magnitude compared with Fig. 1. It can be seen that there is a small jump in the imaginary part of the modeling function at $k_z=0$, which is absent in the map of Eq. (18). This jump is most pronounced at the phase $\psi = \pi/2$ and equals to zero for $\psi = \pi$.

The modeling formula, Eq. (20), in contrast to Eq. (18), has eight instead of six poles. However, four of them are the non-resonant type that we do not count, leaving only four resonance poles (cf. Eq. (19))

$$k_\pm^\pm = \pm\frac{q}{2}\pm\sqrt{\varkappa+\frac{q^2}{4}-\sqrt{\varkappa q^2+\eta}}\,. \tag{22}$$

Unaccounted poles correspond to a change sign from minus to plus before the inner radical in the expression (22).

Next, we perform the inverse Fourier transformation of the function $G(\mathbf{k}_\perp, z, z_0)$, Eq. (20), by the method of the residue theory taking into account these four poles. As a result, we obtain approximate analytical expressions for Green's function $G(\mathbf{k}_\perp, z, z_0)$ in the form

$$G(\mathbf{k}_\perp, z, z_0) = \frac{\pm i}{(2\pi)^2}\left\{\frac{\exp\left(ik_-^-(z-z_0)\right)\left[\varkappa-(k_-^-+q)^2-\eta\exp\left(-i(qz_0+\psi)\right)\right]}{(k_-^- - k_{+-}^-)(k_-^- - k_{++}^-)(k_-^- - k_{-+}^-)}\right.$$
$$\left.+\frac{\exp\left(ik_-^+(z-z_0)\right)\left[\varkappa-(k_-^++q)^2-\eta\exp\left(i(qz_0+\psi)\right)\right]}{(k_-^+ - k_{+-}^+)(k_-^+ - k_{++}^+)(k_-^+ - k_{-+}^+)}\right\}, \tag{23}$$

with the sign $(-)$ for $z>0$, $\varkappa < q^2/4-\eta$ and $(+)$ for $z<0$, $\varkappa \geq q^2/4-\eta$;

$$G(\mathbf{k}_\perp, z, z_0) = \frac{\pm i}{(2\pi)^2}\left\{\frac{\exp\left(ik_+^-(z-z_0)\right)\left[\varkappa-(k_+^-+q)^2-\eta\exp\left(-i(qz_0+\psi)\right)\right]}{(k_+^- - k_{--}^-)(k_+^- - k_{++}^-)(k_+^- - k_{-+}^-)}\right.$$
$$\left.+\frac{\exp\left(ik_+^+(z-z_0)\right)\left[\varkappa-(k_+^++q)^2-\eta\exp\left(i(qz_0+\psi)\right)\right]}{(k_+^+ - k_{+-}^+)(k_+^+ - k_{++}^+)(k_+^+ - k_{-+}^+)}\right\}, \tag{24}$$

with the sign $(+)$ for $z<0$, $\varkappa < q^2/4-\eta$ and $(-)$ for $z>0$, $\varkappa \geq q^2/4-\eta$. Second subscript at $k_{\pm\pm}^\pm$ in Eqs. (23) and (24) shows a sign before the inner radical in Eq. (22).

We use analytical expressions, Eqs. (23) and (24), for the approximate description of the real part of Green's function in the near-field in the gap. At a small amplitude of the superlattice modulation $\Delta\varepsilon/\varepsilon \ll 1$, in the center of the band gap at $\varkappa = q^2/4$, we obtain a simple expression for the real part of Green's function (in

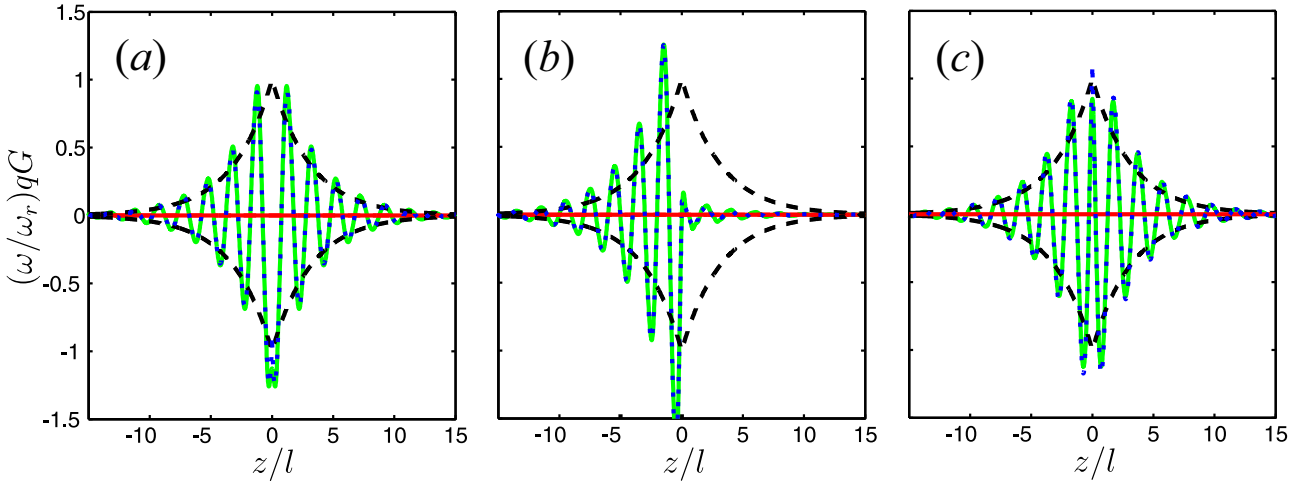

Fig. 8. The normalized Green's function $(\omega/\omega_r)qG(\omega, z)$ in the middle of the first gap ($\nu = q^2/4$) for various values of the superlattice phase $\psi = 0$ (a), $\pi/2$ (b) and π (c): exact values (solid curves, green) and practically coinciding with them the graphs of the approximate equation, Eq. (25) (dashed curves, blue). The graphs of the exponential factor, Eq. (26) (dashed curves, black) are also shown. $\Delta\varepsilon/\varepsilon = 0.4$, $\omega''/\omega_r = 10^{-5}$. (For interpretation of the references to color in this figure caption, the reader is referred to the web version of this paper.)

this case $G''(z, z_0) = 0$)

$$G'(z, z_0) = -\frac{1}{(2\pi)^2}\frac{1}{q}\exp\left(-\frac{|z - z_0|}{l_s}\right)\times\left[\cos\left(\frac{q(z - z_0)}{2} + qz_0 + \psi\right) + \sin\left(\frac{q|z - z_0|}{2}\right) - \frac{2\eta}{q^2}\cos\left(\frac{q(z - z_0)}{2}\right)\right]. \quad (25)$$

where the characteristic decay length

$$l_s \approx \frac{4}{\pi}\frac{l\varepsilon}{\Delta\varepsilon}. \quad (26)$$

For the superlattice with a rectangular modulation of the dielectric permittivity $\varepsilon(z)$ (one-dimensional photonic crystal), the characteristic decay length of the field oscillations in the bandgap was obtained in Ref. [5] as

$$l_d \approx \frac{l}{\log(n_h/n_l)}, \quad (27)$$

where n_h and n_l are the refractive indices of adjacent layers of the crystal and $n_h > n_l$. At small depth of modulation, the ratio n_h/n_l can be expressed by the average value ε and the value of modulation $\Delta\varepsilon$ of the permittivity as

$$\frac{n_h}{n_l} = \left(\frac{\varepsilon + \Delta\varepsilon}{\varepsilon - \Delta\varepsilon}\right)^{1/2} \approx 1 + \frac{\Delta\varepsilon}{\varepsilon}. \quad (28)$$

In this case, an expression for l_d from Eq. (27) follows, which differs from Eq. (26) only by a numerical factor of $\pi/4$ (note that this factor is the same as the coefficient of the first harmonic of the rectangular modulation expansion in Fourier series):

$$l_d \approx \frac{l\varepsilon}{\Delta\varepsilon}. \quad (29)$$

Thus, for any of the considered profiles of the function $\varepsilon(z)$, the decay length of the oscillations in the band gap is inversely proportional to the relative depth of modulation of the permittivity $\Delta\varepsilon/\varepsilon$.

The graphs of Eq. (25) are shown in Fig. 8 for various values of the superlattice phase ψ (dashed curves, blue). This figure also shows the results obtained by the numerical inverse Fourier transform of the precision expression, Eq. (6), (solid curves, green). One can see a good agreement between both these graphs. Furthermore, in Fig. 8 is a graph of the exponential factor in Eq. (25), providing spatial decay of the field (dashed lines, black). It is seen the sharp asymmetry of the intensity of the field at $\psi = 0$, when the point $z=0$ corresponds to the inflection of the function $\varepsilon(z)$, i.e., simulates the center of the interface.

5. Conclusion

We found an analytical solution of the equation in **k**-space for Green's function of the scalar model of electromagnetic waves in a sinusoidal superlattice. It allowed us to get the Green's function in **k**-space, $G(\omega, \mathbf{k}, \mathbf{r}_0)$, a compact expression in the form of quickly converging continued fractions. Green's function in r-space, $G(\omega, \mathbf{r}, \mathbf{r}_0)$, has been found by the Fourier transformation of Green's function $G(\omega, \mathbf{k}, \mathbf{r}_0)$ performed by both numerical and approximate analytical methods.

Next, we investigated in detail Green's functions of a plane radiation source, located in the plane xy, $G(\omega, k_z, z_0)$ and $G(\omega, z, z_0)$, i.e., the integrals over the x_0 and y_0 of the found functions $G(\omega, \mathbf{k}, \mathbf{r}_0)$ and $G(\omega, \mathbf{r}, \mathbf{r}_0)$. It is shown that the relief map of Green's function in **k**-space $G(\omega, k_z, z_0)$ dramatically changes with the position of the plane source z_0 relative to the extremes of sinusoidal modulation of the dielectric permittivity $\varepsilon(z)$. Therefore, from the experimental study of the shape of the peaks of Green's function $G(\omega, k_z, z_0)$, it can be determined whether the source is at the minimum, maximum or inflection of the function $\varepsilon(z)$ (or at intermediate points).

From the analysis of Green's function in **r**-space $G(\omega, z, z_0)$ it showed that radical restructuring of the electromagnetic field in the superlattice occurs with increasing the distance from a plane source $|z - z_0|$. The lines of zeros of Green's function $G(\omega, z, z_0)$ at some points come nearer to each other and chains of islets formed on the relief map of this function in the plane ωz. With increasing the distance $|z - z_0|$, the sizes of islands decrease, their number increases. As a result, the dependencies of Green's function $G(\omega, z, z_0)$ on the frequency ω greatly differ at different distances from the radiation source. This effect can be used to measure as the distance to the internal source and the thicknesses of one-dimensional photonic crystals from the frequency dependence of Green's function at the observation point. It is shown that this is a phase effect which disappears when computing Green's function module (or, respectively, when the radiation power and not the intensity is measured). Green's function in **r**-space $G(\omega, z, z_0)$ was

used also to investigate the changes of the LDOS depending on the position of the radiation source relative to the extremes of sinusoidal modulation of the dielectric permittivity $\varepsilon(z)$.

Approximate expressions for Green's functions $G(\omega, \mathbf{k}, \mathbf{r}_0)$ and $G(\omega, \mathbf{r}, \mathbf{r}_0)$, just in the first and second Brillouin zones of the superlattice and the band gap between the bands were derived. The structure of the fields in these areas, in many cases, is of particular interest and relatively simple approximate analytical formulas allow to analyze the characteristics of this structure. We have studied the features of the spatial decay of the real component of the function $G(\omega, z, z_0)$ in the first bandgap depending on the position of the radiation source relative to the extremes of sinusoidal modulation of the dielectric permittivity $\varepsilon(z)$. It is shown that the near-field Green's function has a sharp asymmetry for the radiation source located at the points of inflection of the function $\varepsilon(z)$.

The effects have been found and studied theoretically in this paper, it can be detected and studied experimentally by the methods of the intensively developing currently nanooptics. Optical and electron-optical methods for the experimental study of nano-emitting sources in heterogeneous structures are intensively developed at present [24–30]. The emission of the particles in the doped material excited by an external laser pulses is studied in these works. In most cases the LDOS is studied, which is proportional to the imaginary part of Green's function in the point of the radiation source. We hope that the results of our work will stimulate further development of experimental methods for studying the structure of electromagnetic fields as well beyond the points of emission.

Appendix A

To investigate Eq. (5), we make the substitution

$$k_z \to k_z + pq,\ p = 0, \pm 1, \pm 2, \ldots. \tag{A.1}$$

Then the problem reduces to the solution of an infinite system of linear equations for the Fourier components of Green's function $G(k_z + pq)$

$$\left[\varkappa - (k_z + pq)^2\right]G_p + \eta\left[e^{i\psi}G_{p-1} + e^{-i\psi}G_{p+1}\right] = -\frac{1}{(2\pi)^3}\exp\left[-i(k_z + pq)z_0\right], \tag{A.2}$$

where the notation $G_p = G(k_z + pq)$ is introduce. We introduce notations for the matrix elements of this system

$$a_p = \varkappa - (k_z + pq)^2, \quad b = \eta e^{-i\psi}, \quad c = \eta e^{i\psi}, \quad f_p = -(2\pi)^{-3}\exp\left[-i(k_z + pq)z_0\right]. \tag{A.3}$$

Then the system of equations (Eq. (A.2)) takes the form:

$$cG_{p-1} + a_pG_p + bG_{p+1} = f_p. \tag{A.4}$$

The idea is to express G_{p-1} and G_{p+1} through G_p and the elements of the matrix elements Eq. (A.3). For this we write the equation for G_{p-1} in the next form:

$$cG_{p-2} + a_{p-1}G_{p-1} = f_p - bG_p, \tag{A.5}$$

The following system of equations for the semi-infinite matrices corresponds to Eq. (A.5):

$$\begin{pmatrix} \cdots & \cdots & \cdots & \cdots \\ \cdots & a_{p-3} & b & 0 \\ \cdots & c & a_{p-2} & b \\ \cdots & 0 & c & a_{p-1} \end{pmatrix}\begin{pmatrix} \cdots \\ G_{p-3} \\ G_{p-2} \\ G_{p-1} \end{pmatrix} = \begin{pmatrix} \cdots \\ f_{p-3} \\ f_{p-2} \\ f_{p-1} \end{pmatrix}. \tag{A.6}$$

The solution G_{p-1} can be represented in the form of ascending continued fractions whose partial denominators are ordinary continued fractions [20,21]. For this a finite system of linear equations is considered

$$\begin{pmatrix} a_1 & b_1 & 0 & \cdots & 0 & 0 & 0 \\ c_2 & a_2 & b_2 & \cdots & 0 & 0 & 0 \\ \vdots & \vdots & \vdots & \vdots & \vdots & \vdots & \vdots \\ 0 & 0 & 0 & \cdots & c_{n-1} & a_{n-1} & b_{n-1} \\ 0 & 0 & 0 & \cdots & 0 & c_n & a_n \end{pmatrix}\begin{pmatrix} x_1 \\ x_2 \\ \vdots \\ x_{n-1} \\ x_n \end{pmatrix} = \begin{pmatrix} r_1 \\ r_2 \\ \vdots \\ r_{n-1} \\ r_n \end{pmatrix}. \tag{A.7}$$

According to the Cramer formula

$$x_n = \frac{\| D_n \|}{\| \Delta_n \|}, \tag{A.8}$$

where $\| \Delta_n \|$ is the determinant of the matrix Eq. (A.7) and $\| D_n \|$ is the same determinant with the replacement of the n-th column by the right-hand side of Eq. (A.7). First, we find an expression for the determinant $\| \Delta_n \|$. We subtract the first column multiplied by b_1/a_1 from the second column, and expand the resulting determinant on the elements of the first row. Continuing this process, we obtain

$$\| \Delta_n \| = a_1\left(a_2 - \frac{b_1c_2}{a_1}\right)\left(a_3 - \frac{b_2c_3|}{a_2} - \frac{b_1c_2}{a_1}\right)\times\cdots \times\left(a_n - \frac{b_{n-1}c_n|}{a_{n-1}} - \frac{b_{n-2}c_{n-1}|}{a_{n-2}} - \cdots - \frac{b_1c_2}{a_1}\right), \tag{A.9}$$

where each of the factors is the continued fraction, composed of the elements of the determinant (we denote a continued fraction with a vertical bar). Next, we calculate the determinant $\| D_n \|$. We subtract the first row of the determinant multiplied by c_2/a_1 from the second row and expand the resulting determinant on the elements of the first column. Continuing this process, we obtain

$$\| D_n \| = a_1\left(a_2 - \frac{b_1c_2}{a_1}\right)\left(a_3 - \frac{b_2c_3|}{a_2} - \frac{b_1c_2}{a_1}\right)\times\cdots \times\left(a_{n-1} - \frac{b_{n-2}c_{n-1}|}{a_{n-2}} - \cdots - \frac{b_1c_2}{a_1}\right)\times\left(r_n - c_n\frac{r_{n-1}}{A_{n-1}|} - \cdots - c_2\frac{r_1}{A_1}\right), \tag{A.10}$$

where $A_1 = a_1$, $A_i = a_i - b_{i-1}c_i/A_{i-1}$, and $i = 2, 3, \ldots, n$. Note, that the expansions (Eqs. (A.9) and (A.10)), differ only in the last factors. Substituting Eqs. (A.9) and (A.10) into Eq. (A.8), we obtain the following result:

$$x_n = \frac{r_n}{A_n|} - c_n\frac{r_{n-1}}{A_{n-1}|} - c_{n-1}\frac{r_{n-2}}{A_{n-2}|} - \cdots - c_2\frac{r_1}{A_1}. \tag{A.11}$$

Doing similar calculations, we find

$$x_1 = \frac{r_1}{B_1|} - b_1\frac{r_2}{B_2|} - b_2\frac{r_3}{B_3|} - \cdots - b_n\frac{r_n}{B_n}, \tag{A.12}$$

where $B_n = a_n$, $B_i = a_i - b_{i+1}c_{i+1}/B_{i+1}$, and $i = n-1, n-2, \ldots, 1$. In our case, $c_i = c$ and $b_i = b$. In accordance with the representations Eqs. (A.11) and (A.12), the functions G_{p-1} and G_{p+1} take the form:

$$G_{p-1} = \frac{f_{p-1} - bG_p}{A_{p-1}|} - c\frac{f_{p-2}}{A_{p-2}|} - c\frac{f_{p-3}}{A_{p-3}|} - \ldots, \tag{A.13}$$

$$G_{p+1} = \frac{f_{p+1} - cG_p}{B_{p+1}|} - b\frac{f_{p+2}}{B_{p+2}|} - b\frac{f_{p+3}}{B_{p+3}|} - \ldots, \tag{A.14}$$

where A_p and B_p now have the form $A_p = a_p - bc/A_{p-1}$ and $B_p = a_p - bc/B_{p+1}$. Substituting Eqs. (A.13) and (A.14) into Eq. (A.4), we obtain G_p in the form:

$$G_p = \frac{f_p - c\left[\frac{f_{p-1}}{A_{p-1|}} - c\frac{f_{p-2}}{A_{p-2|}} - \cdots\right] - b\left[\frac{f_{p+1}}{B_{p+1|}} - b\frac{f_{p+2}}{B_{p+2|}} - \cdots\right]}{a_p - \frac{bc}{A_{p-1}} - \frac{bc}{B_{p+1}}}. \quad \text{(A.15)}$$

Without loss of generality, we can set $p=0$ and write the general expression for the spectral form of Green's function in a compact form of Eq. (6).

References

[1] K. Sakoda, Optical Properties of Photonic Crystals, 2nd ed., Springer-Verlag, Germany, 2004.
[2] J.D. Joannopoulos, S.G. Johnson, J.N. Winn, R.D. Meade, Photonic Crystals: Molding the Flow of Light, 2nd ed., Princeton University Press, USA, 2008.
[3] P. Markos, C.M. Soukoulis, Wave Propagation: From Electrons to Photonic Crystals and Left-Handed Materials, Princeton University Press, USA, 2008.
[4] J.-M. Lourtioz, H. Benisty, V. Berger, J.-M. Gerard, D. Maystre, A. Tchelnokov, Photonic Crystals, Second ed., Springer-Verlag, Germany, 2008.
[5] M. Skorobogatiy, J. Yang, Fundamentals of Photonic Crystal Guiding, Cambridge University Press, USA, 2009.
[6] V.F. Shabanov, S.Ya. Vetrov, A.V. Shabanov, Optika Real'nykh Fotonnykh Kristallov, Izdatel'stvo SO RAN, Russia, 2005.
[7] A. Moroz, Europhys. Lett. 46 (1999) 419.
[8] M. Wubs, A. Lagendijk, Phys. Rev. E 65 (2002) 046612.
[9] E. Yeganegi, A. Lagendijk, A.P. Mosk, W.L. Vos, Phys. Rev. B 89 (2014) 045123.
[10] A. David, H. Benisty, C. Weisbuch, Rep. Prog. Phys. 75 (2012) 126501.
[11] V.A. Ignatchenko, Y.I. Mankov, D.S. Tsikalov, Zh. Eksp. Teor. Fiz. 134 (2008) 706 [JETP 107 (2008) 603].
[12] V.A. Ignatchenko, D.S. Tsikalov, Zh. Eksp. Teor. Fiz. 140 (2011) 268 [JETP 113 (2011) 232].
[13] P.M. Morse, H. Feshbach, Methods of Theoretical Physics, McGraw-Hill, USA, 1953.
[14] M.A. Peterson, Phys. Rev. A 27 (1983) 520.
[15] N.A. Nicorovici, R.C. McPhedran, Phys. Rev. E 49 (1994) 4563.
[16] A.Yu. Val'kov, V.P. Romanov, A.N. Shalaginov, Akust. Zh. 37 (1991) 636.
[17] E.V. Aksenova, V.P. Romanov, A.Yu. Val'kov, Phys. Rev. E 59 (1999) 1184.
[18] E.V. Aksenova, A.Yu. Val'kov, V.P. Romanov, Opt. Spektrosk. 104 (2008) 440 [Opt. Spectrosc. 104 (2008) 391].
[19] V.A. Ignatchenko, D.S. Tsikalov, Solid State Phenom. 233–234 (2015) 47.
[20] V.Y. Skorobogat'ko, Theory of Branching Continued Fractions and Its Applications in Computational Mathematics, Nauka, Russia, 1983.
[21] P.K. Korneev, Vestn. Stavrop. State Univ. 38 (2004) 69.
[22] H. Kogelnik, Bell Syst. Tech. J. 48 (1969) 2909.
[23] S.G. Rautian, Opt. Spektrosk. 104 (2008) 122 [Optics and Spectroscopy 104 (2008) 112].
[24] J.P. Dowling, C.M. Bowden, Phys. Rev. A 46 (1992) 612.
[25] M. Scalora, J.P. Dowling, M. Tocci, M.J. Bloemer, C.M. Bowden, J.W. Haus, Appl. Phys. B 60 (1995) 57.
[26] M.D. Tocci, M. Scalora, M.J. Bloemer, J.P. Dowling, C.M. Bowden, Phys. Rev. A 53 (1996) 2799.
[27] J.M. Bendickson, J.P. Dowling, M. Scalora, Phys. Rev. E 53 (1996) 4107.
[28] F.J. Garcia de Abajo, M. Kociak, Phys. Rev. Lett. 100 (2008) 106804.
[29] M.D. Birowosuto, S.E. Skipetrov, W.L. Vos, A.P. Mosk, Phys. Rev. Lett. 105 (2010) 013904.
[30] L. Novotny, B. Hecht, Principles of Nano-Optics, Second ed., Cambridge University Press, USA, 2012.